BNL-65316

X-RAY INDUCED INSULATOR-METAL TRANSITIONS IN CMR MANGANITES

CONF-971201--

V. KIRYUKHIN[1,*], D. CASA[1], B. KEIMER[1], J.P. HILL[2], A. VIGLIANTE[2],
Y. TOMIOKA[3], Y. TOKURA[3,4]
1) Dept. of Physics, Princeton University, Princeton, NJ 08544
2) Dept. of Physics, Brookhaven National Laboratory, Upton, NY 11973
3) Joint Research Center for Atom Technology (JRCAT), Tsukuba, Ibaraki 305, Japan
4) Dept. of Applyed Physics, University of Tokyo, Tokyo 113, Japan
*) Present Address: Dept. of Physics, 13-2154, MIT, Cambridge, MA 02139

ABSTRACT

In this work we report a study of the photoinduced insulator-to-metal transition in manganese oxide perovskites of the formula $Pr_{1-x}Ca_xMnO_3$. The transition is closely related to the magnetic field induced insulator-to-metal transition (CMR effect) observed in these materials. It is accompanied by a dramatic change in the magnetic properties and lattice structure: the material changes from an insulating charge-ordered canted antiferromagnet to a ferromagnetic metal. We present an investigation of the transport and structural properties of these materials over the course of the transition (which usually takes about an hour to complete). The current-voltage characteristics exhibited by the material during the transition are highly nonlinear, indicating a large inhomogeneity of the transitional state. Possible practical applications of this novel type of transition are briefly discussed. We also report a high-resolution x-ray diffraction study of the charge-ordering in these materials. The temperature dependent charge ordering structure observed in these compounds is more complex than previously reported.

INTRODUCTION

Perovskite manganites of the general formula $A_{1-x}B_xMnO_3$ (where A and B are trivalent and divalent metals, respectively) have recently attracted considerable attention by virtue of their unusual magnetic and electronic properties [1]. These properties result from an intricate interrelationship between charge, spin, orbital and lattice degrees of freedom that are strongly coupled to each other. The parameters of the system can be substantially varied by choosing different A and B in the structural formula and by changing the doping level x. This provides the opportunity to control the value and relative strength of important interactions in these materials and synthesize materials exhibiting a vast variety of experimental phenomena.

The most extensively investigated property of the perovskite manganites is the so-called phenomenon of Colossal Magnetoresistance (CMR) [1]. It can be viewed as a magnetic field induced transition from either paramagnetic semiconducting phase (eg. in $La_{0.7}Ca_{0.3}MnO_3$) or from the insulating charge-ordered phase (eg. in $Pr_{0.7}Ca_{0.3}MnO_3$) to the ferromagnetic metallic phase. The large interest to the CMR phenomenon was generated in part due to the possibility of practical applications in magnetic recording. We have recently reported [2] that in $Pr_{0.7}Ca_{0.3}MnO_3$ the transition from the insulating antiferromagnetic (AFM) to metallic ferromagnetic (FM) state can be driven by illumination with x-rays at low temperature

(T<40K). This transition is accompanied by significant changes in the lattice structure, and can be reversed by thermal cycling. In this work we present the study of x-ray illumination effects on the structural and transport properties of $Pr_{1-x}Ca_xMnO_3$, x=0.3-0.5, and also in $Pr_{0.65}Ca_{0.245}Sr_{0.105}MnO_3$. All these materials undergo the photoinduced insulator-metal transition in a certain region of their magnetic phase diagram. Like the closely related CMR phenomenon, this effect also has potential for practical applications.

The x=0 and x=1 members of the $Pr_{1-x}Ca_xMnO_3$ family are insulating antiferromagnets with the manganese ion in the Mn^{3+} and Mn^{4+} valence states respectively [3]. For intermediate x, the average Mn valence is non-integer and the material is a paramagnetic semiconductor at high temperatures. At low temperatures, a variety of charge and magnetically ordered structures is observed (Fig. 1), Ref. [3, 4]. The ground state of $Pr_{1-x}Ca_xMnO_3$ with x=0.3-0.5 is a charge-ordered antiferromagnetic insulator. The 1:1 charge ordering (CO) of Mn^{3+} and Mn^{4+} ions occurs below T_{CO}=200-230K. It is associated with the corresponding lattice distortion leading to the doubling of the crystallographic unit cell. The CO transition is followed by the Néel transition at T_N=150-170K. Compounds with x=0.3-0.4 undergo an additional low temperature transition at which the system acquires a spontaneous magnetic moment (spin-canting transition). Thus, the low temperature state of $Pr_{1-x}Ca_xMnO_3$ with x=0.3-0.5 is the insulating antiferromagnetic charge ordered state.

Application of a magnetic field to this charge ordered insulating state was found to induce an insulator-metal transition, at which the resistivity changes by more than ten orders of magnitude [4]. The metallic phase is ferromagnetic due to the double-exchange interaction [6] between localized 3d t_{2g} spins (S=3/2) of Mn ions mediated by conduction 3d e_g carriers. Due to the carrier delocalization, charge ordering is destroyed in the metallic phase [7]. The field induced transition is associated with large hysteresis [4, 7]; the x=0.3 compound in fact remains metallic after the field is reduced to zero at low temperature, but reverts to charge-ordered insulating state on subsequent heating above 60K. Inside the hysteresis region, either the insulating or the metallic state is metastable, and external perturbations could, in principle, induce a transition to the ground state phase. We find that x-ray illumination constitutes an example of such an external perturbation that induces a transition to the metallic phase in the hysteretic region of the magnetic phase diagram. This effect, a remarkable example of simultaneous structural, magnetic, and insulator-metal transition, is a clear manifestation of strong coupling between charge, lattice and magnetic degrees of freedom in this system. Interesting in itself, the phenomenon of the photoinduced insulator-metal transition in manganite perovskites also provides a new tool for investigation of the microscopic properties of these intriguing compounds.

EXPERIMENT

Single crystals of $Pr_{1-x}Ca_xMnO_3$ were grown by the floating zone technique described elsewhere [4]. Samples with x=0.3, 0.4, 0.5, and also $Pr_{0.65}Ca_{0.245}Sr_{0.105}MnO_3$ were chosen for the experiment. We have performed simultaneous x-ray diffraction and electrical resistance measurements, so that the structural and transport properties of the sample can be correlated. X-rays were scattered from a polished surface of the sample on which two silver epoxy contacts for resistance measurements were placed. The sample was loaded into a superconducting magnet designed for x-ray diffraction measurements. The experiment was performed on beamline X22B at the National Synchrotron Light Source at Brookhaven National Laboratory. The x-ray energy was 8 keV, and the photon flux was $5\times10^{10}s^{-1}mm^{-2}$.

DISCLAIMER

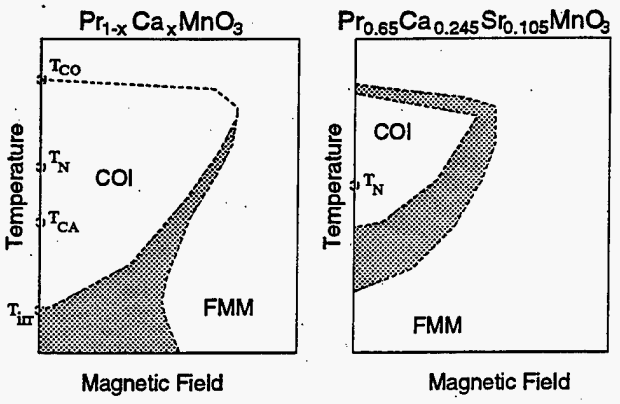

Figure 1: Sketches of the magnetic phase diagram of $Pr_{1-x}Ca_xMnO_3$, $0.3 < x < 0.4$ (left), and of $Pr_{0.65}Ca_{0.245}Sr_{0.105}MnO_3$ (right). The hysteretic regions are shaded. COI - charge ordered insulating phase, FMM - ferromagnetic metallic phase. The values of the relevant temperatures are given in the text. (Adapted from Refs. [4] and [5].)

X-ray measurements were performed in the (H K 0) reciprocal space zone, so that the superlattice reflections due to the lattice distortion accompanying the charge ordering (H K/2 L), K odd, with L=0 could be accessed. (The reflections are indexed on an orthorhombic, though nearly cubic, lattice with room temperature lattice constants a=5.426Å, b=5.478Å, $c/\sqrt{2}$=5.430Å, Ref. [3].) Momentum resolutions of $\sim 0.005 - 0.01$Å^{-1} were achieved. Some of the x-ray measurements, not involving electrical resistivity studies, were performed in a closed cycle refrigerator on beamline X22C. The DC resistance between the contacts deposited on the sample surface was measured by either 2 or 4 contact technique. Supplementary neutron scattering measurements were also conducted. They were performed on the H7 spectrometer at the High Flux Beam Reactor at Brookhaven National Laboratory with 14.7-meV neutrons.

RESULTS

As a $Pr_{1-x}Ca_xMnO_3$, $0.3 < x < 0.5$, sample is cooled through the charge ordering transition, superlattice diffraction peaks appear in the reciprocal space positions (H K/2 L), K odd [3]. The intensity of one such reflection, (4, 1.5, 0), was monitored using neutron diffraction for x=0.3 sample and is shown in Fig. 2 as a function of temperature. The system is in the charge ordered state below T_{CO} ~200K. (The CO peak intensity is slightly depressed below T~100K which is likely the result of spin-canting transition at T_{CA} ~110K, but this effect is small.) As was mentioned in the Introduction, application of the magnetic field drives the system to the metallic state and destroys the charge ordering. This transition is irreversible below T_{irr} ~60K. We find that below T_{irr} x-ray irradiation destroys the charge ordering and induces an insulator-metal transition similar to that driven by the magnetic field.

The effect of x-ray irradiation at T=4K for $Pr_{0.7}Ca_{0.3}MnO_3$ is shown in Fig. 3. Note, that in this and in subsequent figures zero time corresponds to the moment when the resistance becomes measurable (approximately 1 to 3 minutes after the x-rays are switched on). When the sample is being illuminated with x-rays, the charge ordering peak intensity is diminishing, while the conductance is rising. The properties of the sample do not change when the

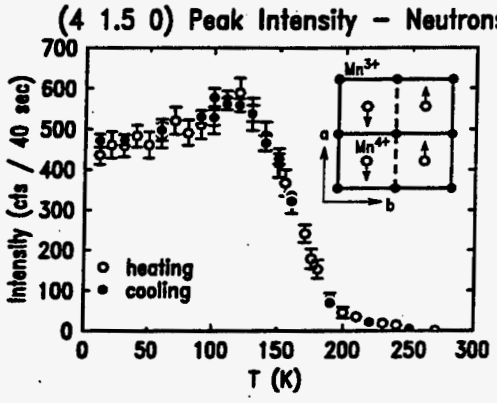

Figure 2: Intensity of the (4, 1.5, 0) superlattice reflection characteristic of the low-temperature charge ordered state of $Pr_{0.7}Ca_{0.3}MnO_3$, measured by neutron diffraction on a single crystal sample. The filled (open) symbols represent data taken on cooling (heating). The inset shows a two-dimensional section of the charge ordering pattern with the primary lattice distortion.

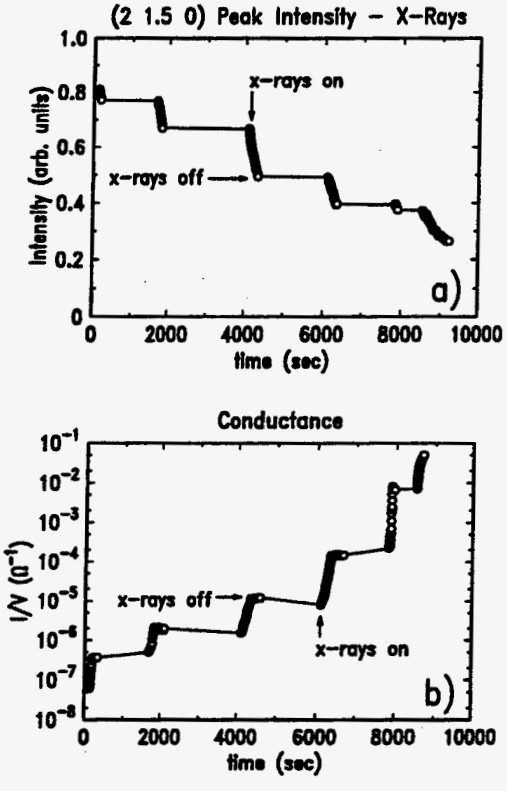

Figure 3: X-ray exposure dependence of the peak intensity of the (2, 1.5, 0) charge ordering superlattice reflection (a), and of the electrical conductance (b) at T=4K in $Pr_{0.7}Ca_{0.3}MnO_3$.

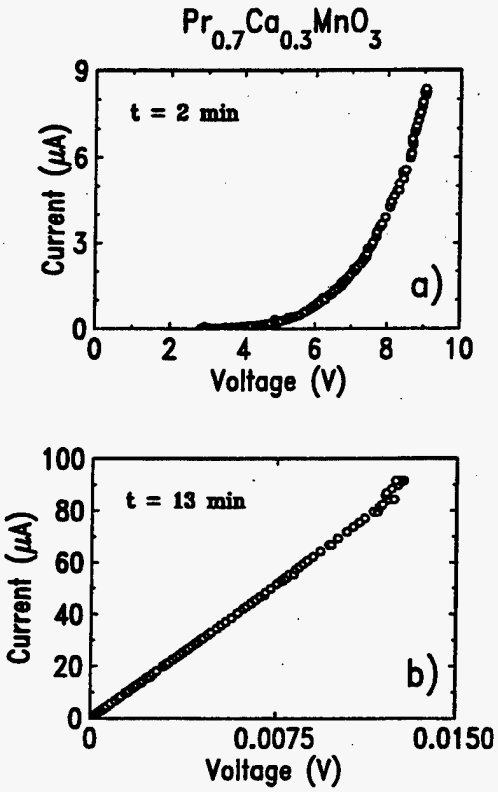

Figure 4: Current-voltage characteristics measured after different x-ray exposures at T=4K.

x-rays are turned off. The transition to the metallic phase is essentially complete after approximately 20 minutes of x-ray irradiation. After that, the sample remains in the metallic phase whether or not x-ray radiation is present.

While the metallic state generated after prolonged x-ray exposure exhibits conventional ohmic conductivity (Fig. 4b), Fig. 4a shows that the current-voltage characteristics after short exposure are remarkably nonlinear (intermediate regime). (We therefore quoted conductance rather than conductivity in Fig. 3.) In this regime, the current-voltage characteristics are often non-reproducible, showing irregular jumps, as shown in Fig. 5. This behavior reflects the inhomogeneity of the intermediate state and is due to formation and destruction of various current paths in the sample. The data of Fig. 5 also shows that application of voltage across the sample (or, equivalently, injection of current carriers into it) drives the system towards the metallic state. A possible explanation of this effect is that when the charge carriers are forcedly moved (delocalized) they revive the ferromagnetic interaction and convert a portion of the sample into the metallic state, producing a new current path. Recently, it was reported that application of the sufficiently large voltage to the $Pr_{0.7}Ca_{0.3}MnO_3$ sample at low temperature converts it into the metallic state [8], providing an argument in favor of this explanation. However, in this case the material stays metallic only as long as the voltage is applied, and reverts to the insulating state when the voltage is reduced to zero.

Due to the finite x-ray penetration depth in this compound, only a narrow surface region should undergo the transition to the metallic phase. We obtain $\rho \sim 5 \times 10^{-4} \Omega cm$ for the ohmic resistivity after prolonged x-ray exposure, using the calculated for our scattering geometry x-ray penetration depth of about $2\mu m$ as the depth of the conducting channel between the contacts. This is (to within the errors) identical to the resistivity measured

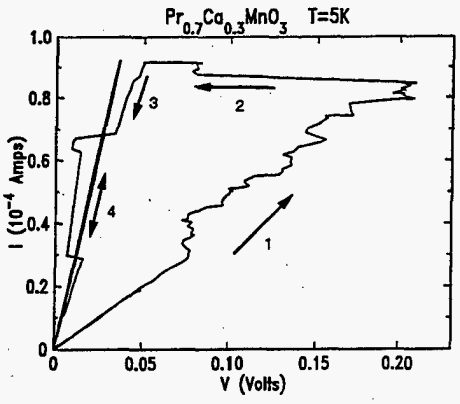

Figure 5: An example of current-voltage characteristics in the intermediate regime. Arrows show the sequence at which the data were taken.

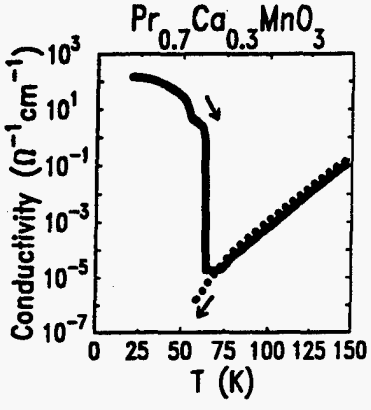

Figure 6: Conductivity measured on cooling before x-ray illumination (dotted curve) and on heating after illumination with x-rays for a moderate amount of time (solid curve). The conductivity on cooling was measured directly. On heating, the conductance data were converted to conductivity by considering a conducting channel produced by the x-ray irradiation described in the text.

without x-rays above the critical magnetic field [4], suggesting that the photoinduced and field-induced metallic phases are identical. Further strong evidence for this assertion comes from a comparison of the metastability boundaries of these two metallic states. Figure 6 shows that the x-ray induced conductivity is annealed out on heating above 60 K, which coincides with the annealing temperature T_{irr} of the magnetic-field-induced phase [4]. Although the magnetization was not measured directly, the close analogy to the magnetic-field-induced transition implies that the magnetic properties of the sample change dramatically with illumination, from canted antiferromagnetic to ferromagnetic. To our knowledge, this is the first example of a photoinduced antiferromagnet-to-ferromagnet transition.

We have studied the effects of x-ray illumination at various temperatures and magnetic fields inside and outside of the hysteretic region of the magnetic phase diagram. Our general conclusion is that in all samples (except for the x=0.5 sample, see below) the x-ray illumination induces the transition to the metallic phase *inside* the hysteretic region; outside of this region we do not observe any measurable changes in the structure or resistivity of the samples. The closer we move to the boundaries of the hysteretic (metastability) region, the harder is to induce the transition. This is reflected in the slower transition rates under the

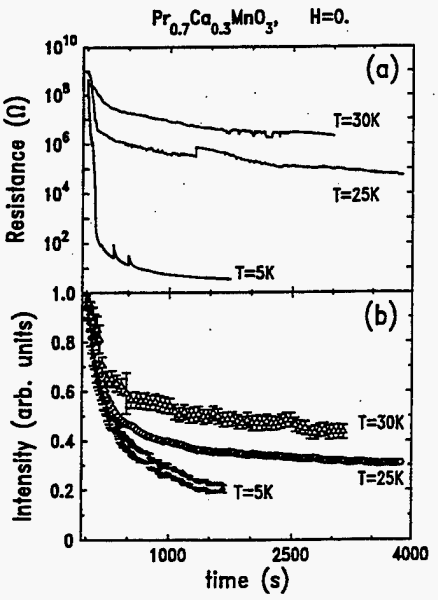

Figure 7: X-ray exposure dependence of the electrical resistance (a), and (2, 1.5, 0) charge ordering peak intensity at various temperatures in zero field in $Pr_{0.7}Ca_{0.3}MnO_3$.

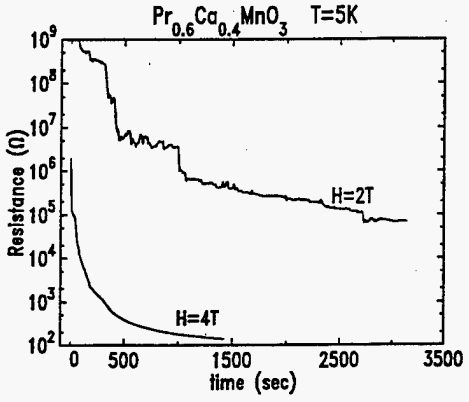

Figure 8: X-ray exposure dependence of the electrical resistance in the $Pr_{0.6}Ca_{0.4}MnO_3$ sample at T=5K in various magnetic fields.

same x-ray flux. This tendency is illustrated by the data of Figs. 7 and 8: the transition proceeds faster at lower temperatures and higher magnetic fields.

In the x=0.5 sample it was possible to induce the insulator-metal transition at low temperatures outside of the hysteretic region of the phase diagram reported in [4]. Namely, the transition is induced at T=5 K, H=8 Tesla. Thus, the boundaries of the metastable region for this sample should be reconsidered. When the magnetic field is turned off, the sample returns to the insulating state at H=0. This transition is not sharp and occurs between 2 and 4 Tesla. The discrepancy between our measurements and those of [4] is probably due to the large times required for the insulator-metal conversion (high energy barrier between the states) at low magnetic fields.

While x-ray irradiation outside of the metastability region does not result in any observable changes in the sample resistance or the CO peak intensity, it nevertheless significantly affects the sample properties. For example, the x=0.4 sample at T=5K undergoes the insulator-metal transition at H~7 Tesla when not subject to x-ray irradiation. But if this

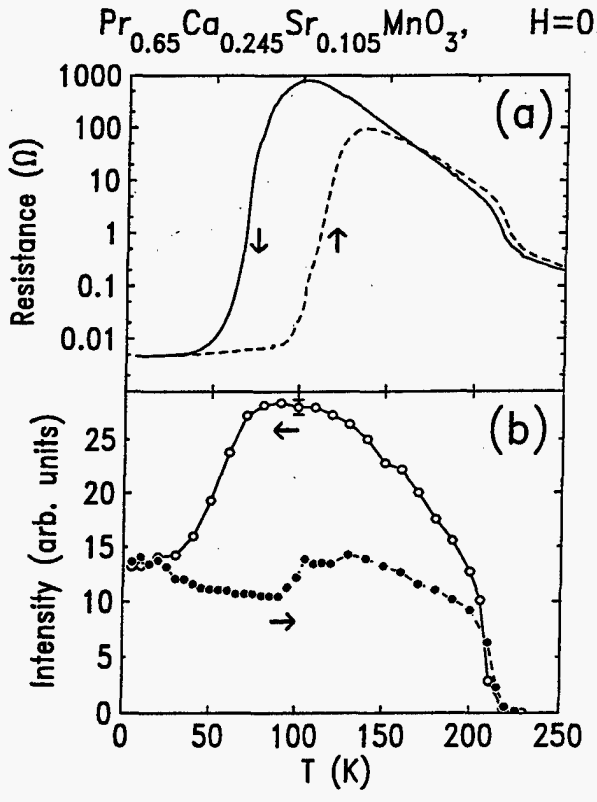

Figure 9: The temperature dependence of the sample resistance (a), and the (2, 1.5, 0) CO peak intensity (b) in $Pr_{0.65}Ca_{0.245}Sr_{0.105}MnO_3$ on heating and on cooling.

sample is irradiated at H=0, T=5K for approximately 10 minutes (and then the x-rays are switched off), it undergoes the transition between 5.0 and 5.5 Tesla. We also find that x-ray irradiation at low temperature and zero field results in faster transition rates when the sample is subsequently irradiated in the field (in the hysteretic region of the phase diagram). Similar effects were observed in the x=0.5 sample. Therefore, x-ray radiation induces changes in the sample also outside of the metastability region of the phase diagram, even though these changes do not reveal themselves in the resistivity or structural measurements.

The last sample we discuss here, $Pr_{0.65}Ca_{0.245}Sr_{0.105}MnO_3$, has its CO phase shifted to higher temperatures (Fig. 1), and the metallic phase is reentrant at low T, Ref. [5]. The temperature dependencies of the electrical resistance and the CO peak intensity for this sample are shown in Fig. 9. Note, that the charge ordering does not disappear in the low temperature metallic phase. Also, contrary to the resilts of Ref. [5], the CO peak intensity does not recover in the insulating phase on heating. This may be the result of the x-ray illumination effects, since the x-ray intensity in our experiment was much higher than that of the Ref. [5]. The nature of the coexisting metallic conductivity and charge ordering is intriguing and will be the subject of the further investigation. We have investigated the x-ray illumination effects in the hysteretic region at H=0, T=70K and T=100K. In both cases, we were able to induce the transition to the conducting phase. The x-ray irradiation effect on the charge ordering was in this case substantially smaller than in $Pr_{0.7}Ca_{0.3}MnO_3$: at T=70K the reduction of the CO peak intensity was about 20% after 5 hours of the x-ray exposure, and at T=100K the reduction was not observed (less than 5%) after 2 hours of irradiation (when the transition to the conducting phase is essentially complete).

In our previous paper [2] we have concluded that the photoinduced transition is caused

by x-ray photoelectrons and secondary electrons generated in collision (such mechanisms as oxygen diffusion, beam heating, and other experimental artifacts were carefully eliminated). The scenario that we proposed was the following. The insulating state in these materials is believed to be associated with strong polaronic self-trapping of the carriers mediated by the Jahn-Teller distortion of the Mn^{3+} ion [9]. In the CO phase, these distortions order, giving rise to the CO diffraction peaks. In the conducting ferromagnetic phase the electrons are delocalized, and the lattice distortion is absent. When an electron gets photoexcited out of the polaronic self-trap, the lattice relaxes, which is unambiguously demonstrated by the data of Fig. 3. The electron does not get captured again since the distortionless conducting phase is (meta)stable. Any means of removal of the electron from the polaronic trap should induce the transition. It was recently shown, that forced carrier injection (application of high voltages) [8], and visible light together with carrier injection [10] also drive the system into the metallic state. However, in these cases the induced conductivity is not persistent. This was attributed to the collapse of the conducting paths due to the elastic strain exerted to them by the insulating matrix [10].

Inhomogeneity and lattice strain seem to play an important role in these materials. It was recently shown that two separate phases associated with the metallic and the insulating phases coexist in the x-ray irradiated material [11]. These phases possess different lattice constants, which results in the lattice strain. These observations, along with the results of [8, 10] and our current-voltage characteristics measurements, demonstrate the inhomogeneity of the photoinduced state in the investigated compounds. Therefore, x-ray irradiation of the sample most likely results in the creation of the FM metallic clusters, and when the percolation threshold is reached, the metallic conductivity is attained. The FM clusters might also be created outside of the hysteretic region (not reaching the concentration necessary for the metallic conductivity), facilitating the transition upon subsequent application of higher magnetic field. This could explain why the field-induced transition occurs at lower fields if the sample is irradiated outside of the metastability region. The authors of [11] have also reported that lattice strain develops below T_{CO} even above the irreversibility temperature T_{irr}. Based on this observation, they proposed that the FM clusters are present in the system at any $T < T_{CO}$, inducing the lattice strain and also being responsible for the ferromagnetic moment below T_{CA}. (Such clusters were observed in different perovskite materials well above Curie temperature [12].) However, recent scanning Hall probe measurements of the surface magnetization contradict this hypothesis [13]. In any case, a complex strained state is realized in these materials at low temperatures. X-ray irradiation creates clusters of the FM phase in the insulating AFM matrix, resulting in a unique example of microscopic phase separation in this system.

In addition to the lattice strain and possible phase separation, the CO state in these materials is more complex than previously reported [3, 11]. Our latest x-ray measurements show that the CO diffraction peaks are split into two components (the peaks are shifted from each other along the (H, H, 0) direction in the reciprocal space). Thus, two different ordering wavevectors are present in the system. One of the components is broader in the q-space than the other, and therefore we denote these peaks as "broad" and "sharp". Their intensities show strikingly different, hysteretic temperature dependencies, as shown in Fig. 10. The behavior of the broad component above T_{irr} is consistent with the neutron diffraction data of Fig. 2, and therefore it may reflect bulk behavior of the material. The sharp component, on the other hand, is almost certainly due to surface effects, unless the properties of the sample are strongly affected by the x-ray irradiation even at these high temperatures. These

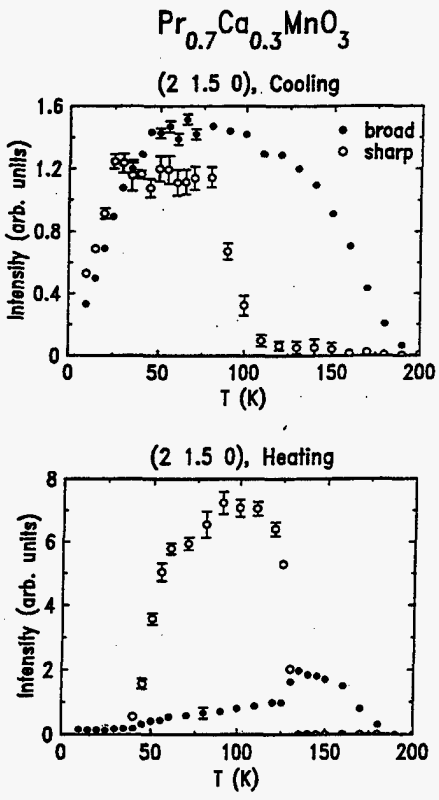

Figure 10: Temperature dependencies of the "broad" and "sharp" components observed in the vicinity of the (2, 1.5, 0) position on cooling and on heating in $Pr_{0.7}Ca_{0.3}MnO_3$.

two peaks can come from different orthorhombic twin domains present in the sample. The observed difference in the scattering angle δq (0.2° at the x-ray energy 8 keV) is roughly consistent with that calculated from the lattice parameters given in [11]. In this case, doubling of the unit cell in both a and b crystallographic directions is present near the surface of the sample. Neither of the two components can come from the suggested FM clusters: δq calculated from the lattice constants of the insulating and the metallic phases [11] at this wavevector (about 0.06° at T=20K) is much smaller than experimentally observed. The data of Fig. 10 is puzzling and demonstrate the complex nature of the lattice distortion near the surface in the CO phase. Surface effects are known to play an important role in manganites (see, for example, the discussion of low-field magnetoresistance in Ref. [1]); more experimental work is needed to understand them in detail. The fact that the surface properties of these materials are different from the bulk ones should be taken into account when investigating low-field tunneling magnetoresistance and other grain boundary related effects. Also, the x-ray data of Ref. [11], including the observation of the lattice strain below T_{CO}, may be affected by the surface effects. We should note that the difference between the bulk and surface properties (including different correlation lengths) was observed before in other materials [14], but remains largely unexplained. To separate the surface and bulk behavior unambiguously, high resolution neutron diffraction measurements are needed.

The observation of the photoinduced insulator-metal transition in CMR manganites opens the way for a variety of further experimental studies. Detailed structural and transport measurements should reveal the microscopic nature of the intriguing low-temperature state of these materials. The understanding of this phase will help to elucidate the physics underlying the complex properties of the manganites. From the point of view of appli-

cations, the unique properties of the manganites may prove useful in x-ray detection and lithography. Using x-ray lithography, it may be possible to pattern very small ferromagnetic structures into these materials, which would open up new possibilities for both fundamental and applied research on magnetism.

CONCLUSIONS

The main result reported in this work is the observation of the x-ray induced transition from the antiferromagnetic charge-ordered insulating into ferromagnetic metallic state. The transition can be induced in the hysteretic (metastable) regions of the magnetic phase diagram of the investigated compounds. Substantial changes in the lattice structure ("melting" of the charge lattice) are observed during the transition. The material can be annealed back into the insulating phase by heating above the irreversibility temperature, T_{irr}. The charge-ordered phase at low temperatures possesses a complex structure, which remains to be understood.

The study of this novel type of transition helps to elucidate the physics responsible for the complex phenomena exhibited by the manganites. First, it illustrates the importance of the electron-lattice coupling thought to be responsible for the transport properties of these materials. Second, it provides clues for understanding of the complex nature of their low-temperature state. Therefore, the discovered effect also provides a useful tool for investigation of the properties of the manganites. Many of these properties are still not understood completely, and new phenomena will certainly be discovered. We believe, that manganite materials will continue to provide a rich ground for both fundamental and applied research in the future.

ACKNOWLEDGEMENTS

The work at Princeton University was supported by NSF grants DMR-9303837 and DMR-9701991, and by the Packard and Sloan Foundations; the work at Brookhaven National Laboratory was supported by the US Department of Energy under contract DE-AC02-98CH10886 ; this work was also supported in part by NEDO and the Ministry of Education, Japan.

References

[1] For a review, see A. P. Ramirez, J. Phys.: Condens. Matter **9**, p. 8171 (1997)

[2] V. Kiryukhin, D. Casa, J. P. Hill, B. Keimer, A. Vigliante, Y. Tomioka, and Y. Tokura, Nature **386**, p. 813 (1997)

[3] Z. Jirak, S. Krupicka, Z. Simsa, M. Dlouha, and S. Vratislav, J. Magn. Magn. Mat. **53**, p. 153 (1985)

[4] Y. Tomioka, A. Asamitsu, H. Kuwahara, Y. Moritomo, and Y. Tokura, Phys, Rev. B **53**, p. R1689 (1996)

[5] Y. Tomioka, A. Asamitsu, H. Kuwahara, and Y. Tokura, J. Phys. Soc. Japan **66**, p. 302 (1997)

[6] C. Zener, Phys. Rev. **82**, p. 403 (1951); P. W. Anderson and H. Hasegava, Phys. Rev. **100**, p. 675 (1955)

[7] H. Yoshizawa, H. Kawano, Y. Tomioka, and Y. Tokura, Phys. Rev. B **52**, p. R13145

[8] A. Asamitsu, Y. Tomioka, H. Kuwahara, and Y. Tokura, Nature **388**, p. 50 (1997)

[9] A. J. Millis, P. M. Littlewood, and B. I. Shraiman, Phys. Rev. Lett. **74**, p. 5144 (1995)

[10] K. Miyano, T. Tanaka, Y. Tomioka, and Y. Tokura, Phys. Rev. Lett. **78**, p. 4257 (1997)

[11] D. E. Cox, P. G. Radaelli, M. Marezio, S-W. Cheong, Phys. Rev. B **57**, to be published

[12] J. W. Lynn, R. W. Erwin, J. A. Borchers, Q. Huang, A. Santoro, J-L. Peng, and Z. Y. Li, Phys. Rev. Lett. **76**, p. 4046 (1996); J. M. De Teresa, M. R. Ibarra, P. A. Algarabel, C. Ritter, C. Marquina, J. Blasco, J. García, A. del Moral, Z. Arnold, Nature **386**, p. 256 (1997)

[13] D. Casa, K. Moler, B. Keimer, Y. Tomioka, and Y. Tokura, unpublished

[14] S. R. Andrews, J. Phys. C **11**, 3721 (1986); T. R. Thurston, *et al.*, Phys. Rev. Lett. **70**, 3151 (1993); Q. J. Harris, *et al.*, Phys. Rev. B **52**, 15420 (1995); G. M. Watson, *et al.*, Phys. Rev. B **53**, 686 (1996)

Report Number (14) BNL--65316
CONF-971201--

Publ. Date (11) 199712
Sponsor Code (18) DOE/ER, XF
UC Category (19) UC-404, DOE/ER

DOE